

Velocity vectors of a quiescent prominence observed by Hinode/SOT and the MSDP (Meudon)

B. Schmieder¹ R. Chandra¹ A. Berlicki² and P. Mein¹

¹ Observatoire de Paris, LESIA, UMR8109 (CNRS), F-92195 Meudon Principal Cedex, France
e-mail: brigitte.schmieder@obspm.fr

² Astronomical Institute, Academy of Sciences, Ondřejov, Czech Republic
Astronomical institute, University of Wrocław, Poland

Received ———; accepted ———

ABSTRACT

Context. The dynamics of prominence fine structures is a challenge to understand the formation of cool plasma prominence embedded in the hot corona.

Aims. Recent observations from the high resolution *Hinode*/SOT telescope allow us to compute velocities perpendicularly to the line-of-sight or transverse velocities. Combining simultaneous observations obtained in $H\alpha$ with *Hinode*/SOT and the MSDP spectrograph operating in the Meudon solar tower we derive the velocity vectors of a quiescent prominence.

Methods. The velocities perpendicular to the line-of-sight are measured by time slice technique, the Dopplershifts by the bisector method.

Results. The Dopplershifts of bright threads derived from the MSDP reach 15 km s^{-1} at the edges of the prominence and are between $\pm 5 \text{ km s}^{-1}$ in the center of the prominence. Even though they are minimum values due to seeing effect, they are of the same order as the transverse velocities.

Conclusions. These measurements are very important because they suggest that the vertical structures shown in SOT may not be real vertical magnetic structures in the sky plane. The vertical structures could be a pile up of dips in more or less horizontal magnetic field lines in a 3D perspective, as it was proposed by many MHD modelers. In our analysis we also calibrate the *Hinode* $H\alpha$ data using MSDP observations obtained simultaneously.

Key words. Solar prominence, spectroscopy, space observations

1. Introduction

The existence of cool structures in so called prominences and filaments during a few solar rotations embedded in the hot corona has been a mystery since the beginning of their spectrographic observations (d’Azambuja & d’Azambuja, 1948). Many reviews concerned the study of quiescent prominences (Schmieder, 1989; Tandberg-Hanssen, 1994; Labrosse et al., 2009; Mackay et al., 2009). Since that time period, it is a challenge to derive what is the best mechanism to succeed to maintain cool plasma in the corona. A very popular idea is that the plasma is frozen in magnetic field lines and stays cool due to the low transverse thermal conduction (Démoulin et al., 1989). Many magnetic and static models have been developed on this idea (Kuperus & Raadu, 1974; Kippenhahn & Schlüter, 1957; Aulanier & Démoulin, 1998; Dudík et al., 2008). But a big question remains: how to get cool plasma inside the field lines into the corona and how to keep it there? It is recognized that this material should come from the chromosphere by levitation or by injection (Saito & Tandberg-Hanssen, 1973). Sufficient mass should be extracted from the chromosphere by magnetic forces which inject or lift the plasma or by pressure forces which evaporate the plasma and then cool it to prominence temperatures. Many models have been developed in this sense, i.e. thermal non-equilibrium models (Mariska & Poland, 1985; Karpen et al., 2003, 2005). Levitation models are proposed through possible magnetic reconnection (van Ballegoijen & Martens, 1989). Injection models could be

due to injection through the reconnection of magnetic field during canceling flux. These models indicate that the plasma in prominences should have a large dynamics and static models may be obsolete. Recent observations at the Swedish Solar Telescope (SST) show highly dynamic plasma in filament threads (Lin et al., 2003, 2005). It was also a first attempt to compute the velocity vectors of the filament threads. They conclude that the threads inclination from the horizontal were around 16 degrees with a net flow in both directions of 8 km s^{-1} . Fine counterstreaming flow is often observed along horizontal threads or in the barbs (Zirker et al., 1998; Schmieder et al., 1991, 2008). *Hinode*/SOT movies (available with the electronic version of the paper) reveal strong dynamics in the prominence fine structures. The spicules close to the barbs could allow to inject plasma inside the fine threads. Is that sufficient to feed continuously the main core of the prominence? A mass budget should be done. Using *Hinode* observations at the limb Berger et al. (2008) and Chae et al. (2008) tried to answer these questions. They reported different velocity measurements. Berger et al. (2008) found upflows of dark bubbles around 20 km s^{-1} and down flows of bright knots less than 10 km s^{-1} looking at Ca II H images in the line center. Chae et al. (2008) analysed an hedgerow prominence and found horizontal displacements before observing downflows of bright knots suggesting the existence of vortex motions.

Prominence dynamics at the limb look quite different from filament dynamics on the disk. The integration along the line of sight complicates the interpretation. Mein & Mein (1991)

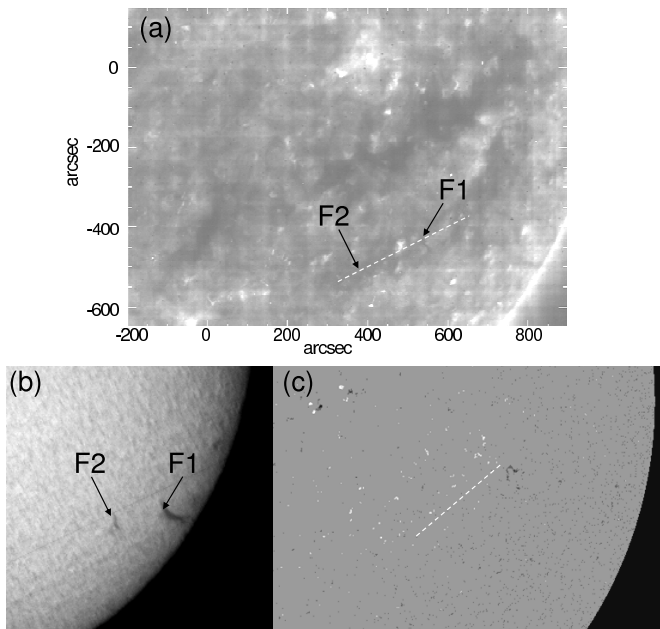


Fig. 1. (a) EIT 304 Å image observed on April 20, 2007 at 01:00 UT, the field of view is 1100×750 arcsec, (b) Filament observed in $H\alpha$ at Meudon on April 22, 2007 at 15:28 UT, (c) MDI longitudinal magnetic field on April 21 at 08:00 UT. The magnetic inversion line is represented by the dashed line in the middle of the EUV filament channel and in MDI image. The letters F1 and F2 indicate approximately the location of the two filament fragments visible in $H\alpha$.

show that more than 15 threads may be integrated along the line of sight and the resulting velocities should depend on two different Gaussian distributions. At the edges of prominences the velocity values are higher because fewer threads are integrated and velocity cells are larger than intensity knots revealing that **bunches** of threads may move with the same velocity plasma (Dopplershifts). Similar results have been found from completely different approaches. Therefore to reproduce Lyman line profiles observed by SOHO/SUMER, Guńár et al. (2007) introduce 10 threads perpendicularly to the line-of-sight with a random velocity distribution in a 2D non LTE radiative transfer code.

We proposed in this study to study both the velocity perpendicular to the line of sight using one hour of observations of *Hinode*/SOT in $H\alpha$ combined with Dopplershifts observed also in $H\alpha$ with the Multichannel Subtractive Double Pass spectrograph (MSDP) operating in the Meudon solar tower. These observations were obtained simultaneously during a coordinated observing program (JOP178). It is the first time that using *Hinode* data such fine structures are resolved in prominences and that oscillations and transverse velocities can be derived (Okamoto et al., 2007; Berger et al., 2008; Chae et al., 2008). *Hinode* has a much better spatial resolution than MSDP by a factor of 5, but the MSDP observations are very useful to calculate the Dopplershifts and to calibrate the intensity of *Hinode*/SOT observations.

2. Observations

The observations presented here were obtained during a coordinated campaign of prominence observations involving *Hinode*, SOHO and TRACE missions, as well as sev-

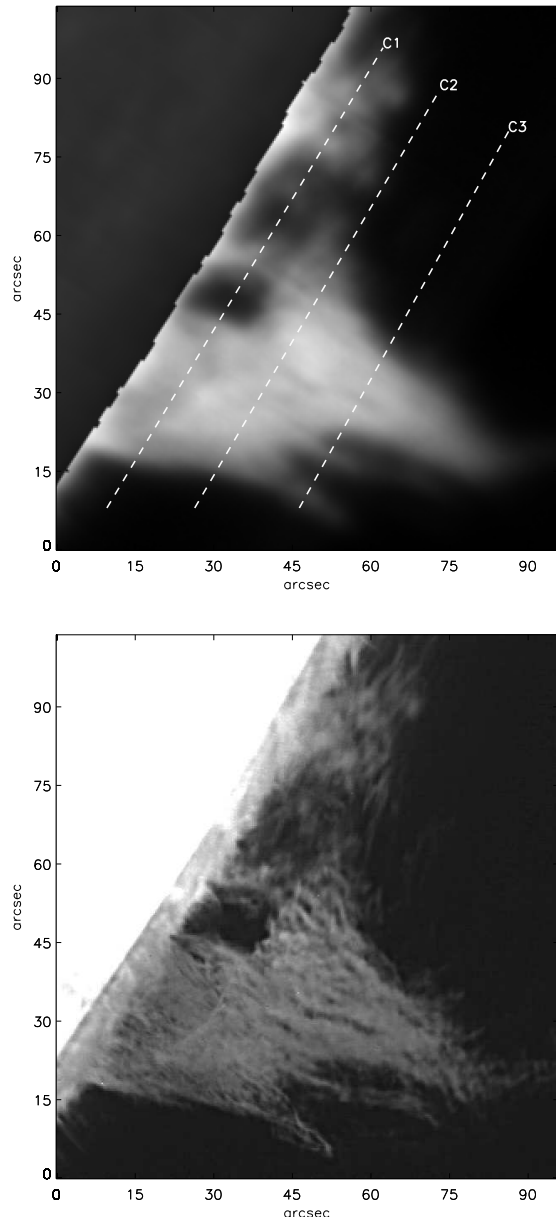


Fig. 2. Top panel: Observation of the prominence in $H\alpha$ line center by the MSDP spectrograph at 13:19:56 UT. Bottom panel: $H\alpha$ image of prominence with *Hinode*/SOT at 13:19:50 UT on 25 April 2007. The 3 cuts used for the calibration are indicated in the top panel.

eral ground-based observatories. These observations were performed in the JOP 178 framework between April 23–29 2007 during the first SUMER-*Hinode* observing campaign. JOP 178 has run successfully many times in the past (see <http://bass2000.obs-mip.fr/jop178/index.html>). JOP 178 is dedicated to the study of prominences and filaments, investigating various aspects such as their three-dimensional structure and their magnetic environment from the photosphere to the corona. The observations of the cavity of the prominence principally by *Hinode*/XRT and TRACE have been described in details by Török et al. (2009) and Heinzel et al. (2008). The prominence is difficult to observe on the disk. Two fragments, F1, F2 have been observed on April 21 and 22 2007 in $H\alpha$ survey spectro-

heliograms of Meudon (Fig. 1). On April 21 they are located at S 33, W 40-50 degree for F1 and S 35 W 35 degree for F2. F1 with a ‘Y’ shape has one branch aligned along a parallel and the other is inclined. It crosses the limb on April 25. The angle P is negative, the leading part of F1 was in the south compared with the following part F1 as crossing the limb. These two fragments are the denser parts of a filament and look to be the feet, the main body is less dense and not visible on the survey observations as it is commonly described (Malherbe, 1989). EIT observes a large dark filament channel on April 21 between an area of positive magnetic flux in the North and negative polarities in the South. The longitudinal magnetic flux is less than ± 10 G. It is difficult to derive the polarity inversion line even when the filament is in the middle of the west quadrant on April 20 (Fig. 1). This prominence is a very quiescent prominence.

2.1. Hinode/SOT observations

The *Hinode* mission is operating since October 2006 (Kosugi et al., 2007). The prominence under study was well observed by the *Hinode*/SOT instrument between 13:04 and 13:59 UT in $H\alpha$ and in Ca II H lines on April 25, 2007. The 50 cm diameter SOT can obtain a continuous, seeing-free series of diffraction-limited images in 388-668 nm range with 0.2–0.3 arcsec spatial resolution. The field-of-view of CaII H line is smaller (108×108 arcsec) and does not cover the whole prominence. We are using in our study only $H\alpha$ images (160×160 arcsec) registered as a 1024×1024 pixels matrix, each pixel having dimensions of 0.16×0.16 arcsec. **The SOT NFI filter is centered on the $H\alpha$ line (as determined in a line scan calibration prior to the observations) with a bandpass width of 120 mÅ.** Prominence with Dopplershifts larger than 20 km s⁻¹ can not be observed because the maximum intensity would be out of the bandpass. The center of the field-of-view in solar coordinates was $[830, -510]$ arcsec and the exposure time was 300 ms. The images have been dark-subtracted and flat-fielded to remove CCD fringes in the $H\alpha$ images (Fig. 2). The images have been sharpened by an unsharp mask procedure in order to increase the fine structure contrast. Looking at the $H\alpha$ SOT movie, we observe that the fine structures of the prominences evolved very rapidly, principally the round-shaped structures, dark “bubbles” at the bottom of the prominence. They are rising and with their half circle shapes. The material in the prominence lying above these dark features are very dynamic as these features are moving up. The material in the bright structures appear to move down. We notice from time to time brighter threads surrounding the top of the bubbles with accelerated velocities. The dynamics of this prominence is comparable to the hedgerow prominence described by Berger et al. (2008).

2.2. MSDP observations

The prominence has been observed during three consecutive days, on the April 24, 25, 26 with the Multichannel Subtractive Double Pass spectrograph (MSDP) operating in the solar tower of Meudon. On April 25 the prominence was observed between 12:09 and 13:32 UT. The entrance field stop of the spectrograph covers an elementary field-of-view of 72×465 arcsec with a pixel size of 0.5 arcsec. The final field-of-view of the images is 500×465 arcsec. The exposure time is 250 ms. We performed consecutive sequences of 60 images with a cadence of 30 sec. The spatial resolution is estimated to be between of 1 arcsec and 2 arcsec depending on the seeing. Using the MSDP tech-

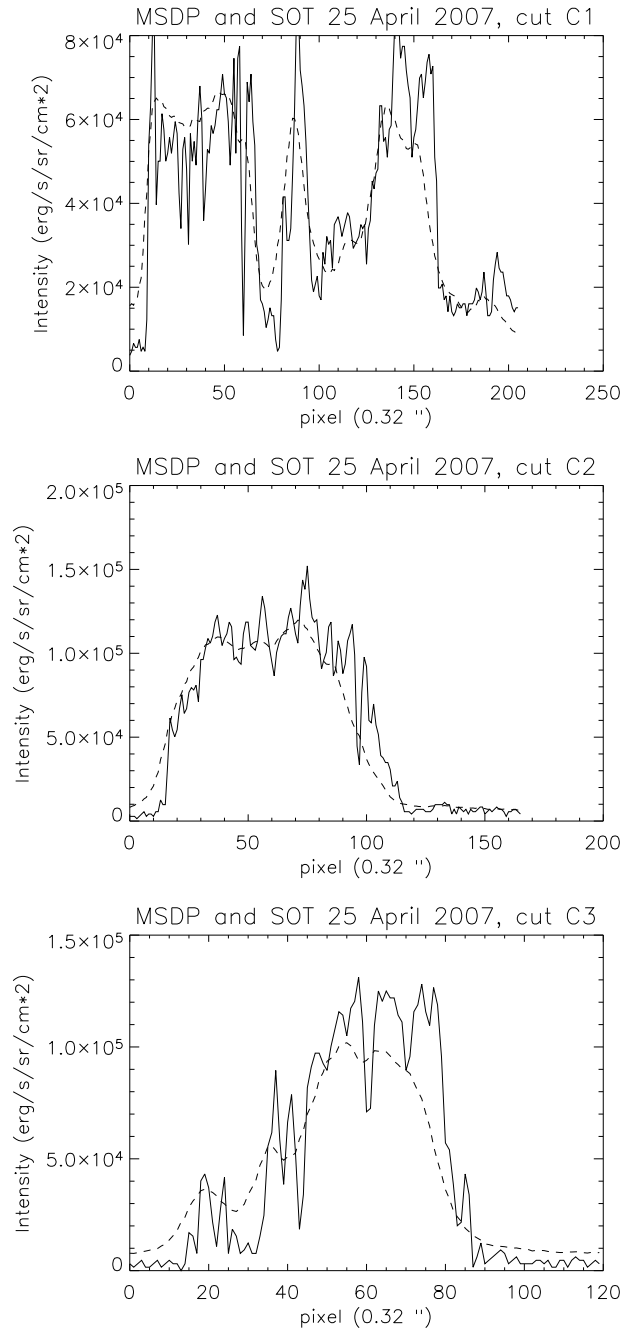


Fig. 3. Calibrated intensities of cuts (dashed lines) through the prominence parallel to the limb observed by MSDP from the South to the North overlaid by cuts (solid lines) obtained through the SOT image of the same prominence at the same time (13:19 UT) for 3 different altitudes 7.5, 18.7, 30 Mm above the solar limb. Cuts 1 is below the main prominence and crosses the bubbles. It is more extended than the other cuts. The cut locations are indicated in Fig. 2.

nique (Mein, 1977, 1991) the $H\alpha$ image of the field-of-view is split in wavelength into nine images covering the same field of view. The nine images are recorded simultaneously on a CCD Princeton camera. Each image is obtained in a different wavelength interval. The wavelength separation between the center wavelength of one image to the next is 0.3 Å. By interpolating with spline functions between the observed intensity in these im-

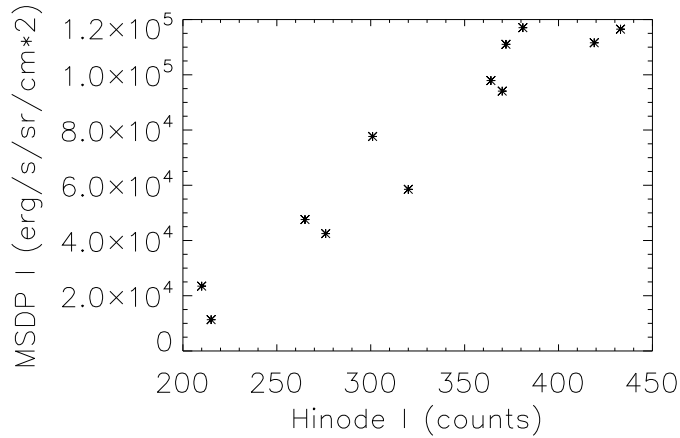


Fig. 4. Counts of the $H\alpha$ SOT intensity versus calibrated MSDP integrated intensity in ergs/s/sr/cm^2 . The plot shows linear behaviour.

ages, we are able to construct $H\alpha$ profiles in each point of the observed field-of-view. A mean or reference disk profile is obtained by averaging over a quiet region on the disk in the vicinity of the prominence (this case at $\sin\theta = 0.98$). The photometric calibration is done by fitting the reference profile to standard profiles for the quiet Sun (David, 1961). We corrected the profile of the scattering light by looking at the nearby corona. The observations of the prominence in $H\alpha$ line center by the MSDP spectrograph are easily coaligned with the $H\alpha$ SOT images obtained at the same times (Fig. 2).

2.3. Normalization of the $H\alpha$ intensities

The normalization of $H\alpha$ intensity allows the comparison of observations with the theory provided by radiative transfer codes (Gouttebroze et al., 1993; Heinzel et al., 2005) leading to the determination of physical quantities of prominences. This is not the scope of this paper. Nevertheless it is interesting to calibrate the *Hinode* data using the MSDP data. The intensities of the MSDP observed profiles are normalized to the local continuum $I_\lambda / (I_{c,loc})_{obs}$, the intensities of the local continuum to the continuum at the disk center $I_{c,loc} / (I_c)$. The continuum at disk center in the wavelength region close to the $H\alpha$ line is (David, 1961): $I_c = 4.077 \times 10^{-5} \text{ erg cm}^{-2} \text{ s}^{-1} \text{ sr}^{-1} \text{ Hz}^{-1}$

To perform the normalization we must apply two corrections : (i) one due to the limb darkening, the reference profiles are measured on the disk near the limb at $\sin(\theta) = 0.98$. It reduces the intensity by a factor 0.547, (ii) the second one taking into account the θ angle, the central intensity is no longer equal to 16% of the intensity of the continuum but is equal to 22.6 % of the intensity of the continuum for $\sin(\theta) = 0.98$. We present cuts drawn parallel to the limb at 3 different altitudes over the limb through the MSDP prominence (see the positions of the cuts in Fig. 2 top panel). The SOT prominence cuts at the same positions have been over-plotted to the MSDP cuts (the bubbles have a contrast between 70 to 90 %) (Fig. 3). The MSDP cuts are smooth with lower contrasts compared to SOT cuts because of the seeing. This allows us to calibrate $H\alpha$ SOT observations. This is valid with some possible translation **according to the accuracy of the wavelength determination**. Using the count numbers of the SOT Level-1 file, we derive the calibration curve shown in

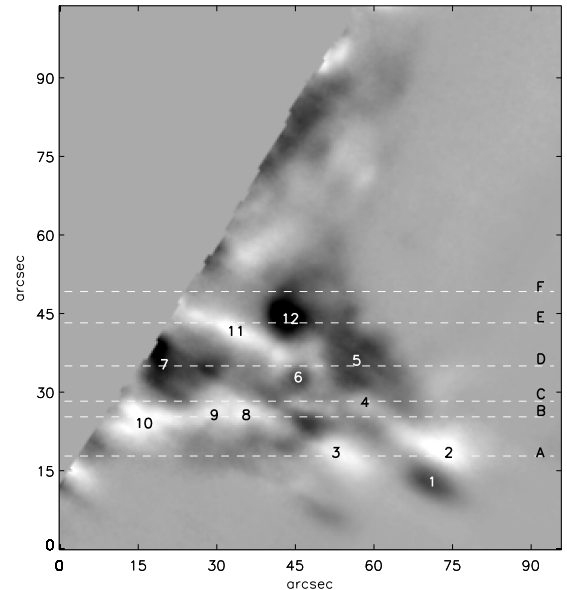
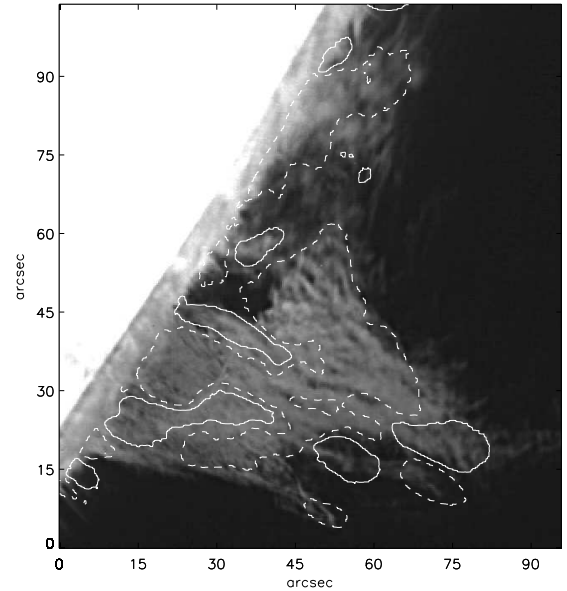


Fig. 5. Top: $H\alpha$ *Hinode*/SOT image at 13:19 UT overlaid by Dopplershift contours, bottom: Dopplershift map of MSDP data at the same time. White/black areas (solid/dashed lines) correspond respectively to blue/redshifts. The dashed straight lines in the bottom image are the location of the slices used to compute the transverse velocity (A to F). The numbers are the points where Dopplershifts have been computed (see Table 1). Some profiles have been drawn in Fig. 6.

Fig. 4. The integrated $H\alpha$ intensity of bright threads are around $1.5 \times 10^5 \text{ ergs/s/sr/cm}^2$.

3. Dopplershifts

A Dopplershift map is presented in Fig. 5. We notice the trend of the velocity pattern with more or less a succession of vertical blue and redshifts elongated cells/ strands. We compute the velocity $V(y)$, in a reference system (x, y, z) , (x, z) being the plane of the sky. We use for that computation the bisector method at the

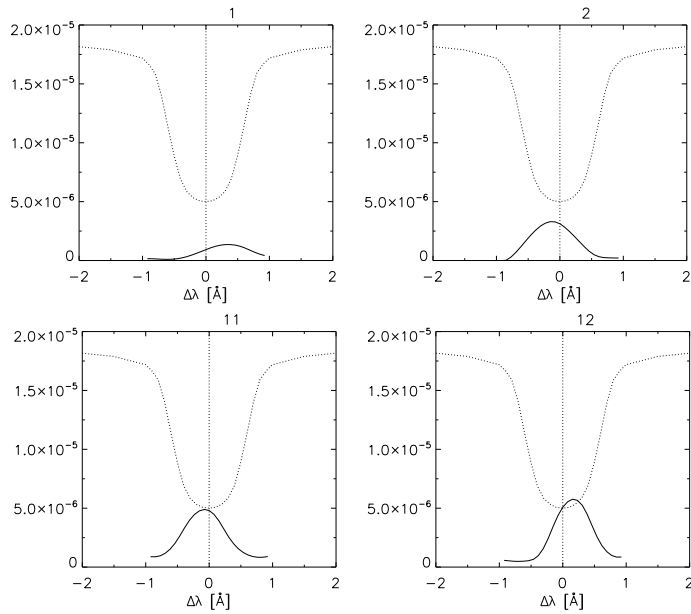


Fig. 6. Profiles of the $H\alpha$ line in different points of the prominence observed with the MSDP at 13:19 UT (in $\text{ergs/s/sr/cm}^2/\text{Hz}$). The numbers at the top of panels correspond to the points marked in Fig. 5. The intensities of profiles of the prominences (solid lines) have been multiplied by a factor 3 and compared with the reference line profiles observed on the disk. The scale in y-axis refers to reference profiles (dotted lines).

inflection point of the line profile ($\pm 0.45 \text{ \AA}$). The trend of this pattern evolves in an hour of observations. Close to the top of the prominence we measure counterstreaming with redshifts of 15 km s^{-1} and blue shifts of -5.5 km s^{-1} (Table 1). In the central part of the prominence the velocity is between ± 1 to $\pm 4 \text{ km s}^{-1}$. At the top of the bubble bright threads move with a velocity of 7 km s^{-1} . The location of the points mentioned in Table 1 are indicated on the Fig. 5. The profiles of the $H\alpha$ line are all relatively narrow (Fig. 6). This means that the different threads along the line of sight have similar velocity **but they still have somewhat lower values due to the smearing and seeing effects**. This should also be true for threads close to each other in the same pixel. It is difficult to estimate the filling factor. Fine structures are tied in **bunches**. This remark has been already done for previous observations (Mein and Mein 1991).

4. Velocity perpendicular to the line-of-sight

The *Hinode* movie shows tremendous downflows mainly for the bright threads and upflows for the dark cavities, ‘bubbles’ rising from the solar limb. This prominence has a similar behaviour as the prominence observed in Ca II H by Berger et al. (2008). The time slice technique (Lin et al., 2005) allows us to get quantitative values of the velocities $V(x,z)$ or $V(\text{trans})$ in the sky plane for different locations in the prominence observed by SOT. We adopt slices of 5 pixels (equivalent to $0.8''$) with the East-West orientation (see Fig. 5, bottom). They follow nearly the common orientation of the fine structures of the prominence. The maximum angle between the East-West direction and the fine structures orientation is equal to 30 degrees. For these structures the measured velocities should be multiplied by a factor 1.25. We did not apply systematically this correction because for each thread, the angle is different and Dopplershifts are also lower values.

Table 1. Dopplershifts $V(\text{Doppler})$ or $V(y)$ and transverse velocities $V(\text{trans})$ or $V(x,z)$ in 12 points in the prominence observed with SOT and the MSDP spectrograph. The 12 points correspond to the named points in Fig. 5 and 7, numbers are for MSDP data and letters are for SOT data. Positive/negative Dopplershifts, $V(\text{Doppler})$ are red/blueshifts, positive/negative transverse velocity, $V(\text{trans})$ are up/down flows. The last column is the norm of the velocity vector.

point MSDP	$V(\text{Doppler})$ km s^{-1}	$V(\text{trans})$ km s^{-1}	point SOT	$ V $ km s^{-1}
1	+15	–	–	15
2	-5.5	-6	A2	8.5
3	-6.7	-2	A1	7
4	-0.6	+4	C	4
5	+1.8	-3	D2	3.5
6	+1.0	-2	D1	1.4
7	+3.0	–	–	3.0
8	-1.8	+3	B3	3.5
9	-1.8	+3	B2	3.5
10	-3.7	-2	B1	4.2
11	-3.6	+9	E1	9.7
12	+7.4	-11	E2	13.2

It appears that many structures in the time-slice diagrams (pixels close to each other along a slice) have the same velocity. A few of the threads show a unique behaviour. Those threads have in general higher velocities, reaching -10 km s^{-1} for a short time (5 to 10 minutes). The other ones have commonly a velocity of the order of -2 to -6 km s^{-1} . The trend is downflows for the bright structures. The transverse velocity $V(x,z)$ and the norm of the velocity vector $\sqrt{[(V(y))^2 + V(x,z)^2]}$ are indicated in Table 1. According to the velocity vector, the fine structures would be not really vertical but inclined from the vertical by an angle between 30 degrees to 90 degrees. Some pixels exhibit upflows and later down flows. We identify these motions as stationary waves with periods of ten to twenty minutes. If we consider that these pixels belong to vertical structures, the plasma is oscillating along/in the structures, if we consider the structures horizontal, the structures themselves oscillate like the Okamoto et al. (2007) transverse waves. Fig. 7 shows the transverse velocities.

5. Discussion and Conclusion

For the first time an $H\alpha$ hedgerow prominence has been observed simultaneously by a high spatial resolution telescope (*Hinode*/SOT) and by a spectrograph (MSDP) operating in the Meudon solar tower on April 25 2007. *Hinode*/SOT allows us to get the velocities perpendicular to the line-of-sight $V(x,z)$. The second – the line-of-sight velocities $V(y)$ derived from Dopplershifts. The prominence shows strong dynamics in the SOT movie with dark cavities rising from the limb with an upward velocity reaching 24 km s^{-1} and downflowing vertical-like bright threads. These threads are moving horizontally to avoid the dark cavities. During the rise of cavities, ahead of them, are observed bright curved fine structures from time to time with high velocities similar to the speed rise of the bubble. The *Hinode*/SOT observations have been calibrated by using the MSDP data. The integrated $H\alpha$ intensity of the threads reaches $1.5 \times 10^5 \text{ ergs/s/sr/cm}^2$. The contrast of the dark cavities is between 70 and 90%.

The transverse velocities $V(x,z)$ of the bright threads are computed by time slice technique and these values are of the or-

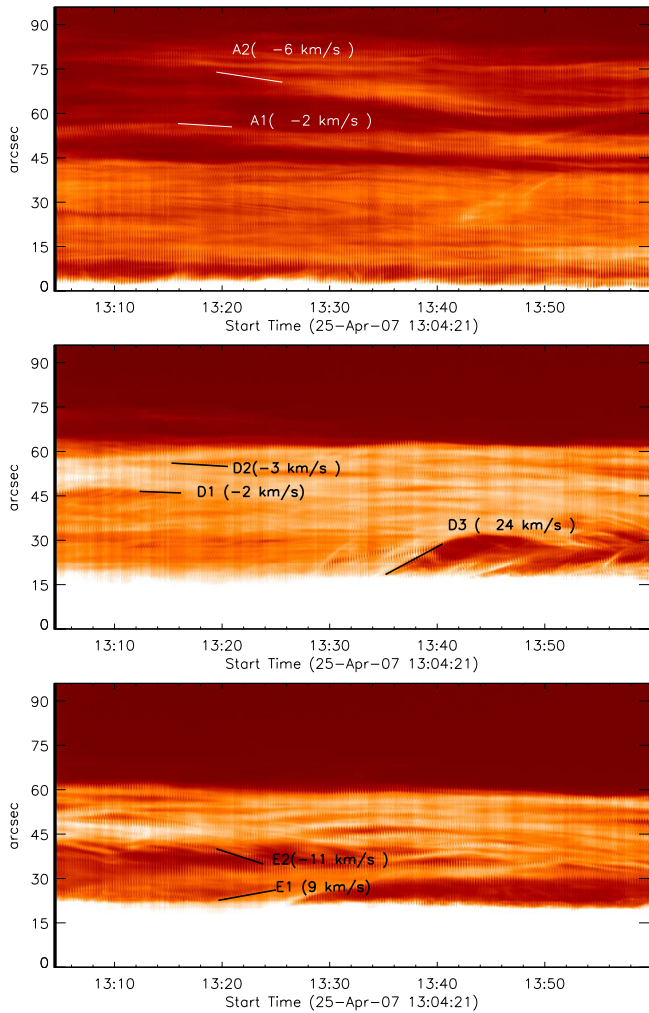


Fig. 7. Transverse velocities in SOT bright structures using time slice technique (axis x unit is time, axis y unit is arc sec along the slide). Top/medium/bottom frame corresponds to slice A/ D/ E, drawn in Fig. 5. They show the velocities measured respectively in points A1, A2, D1, D2, E1, E2 (Table 1). Positive/negative velocities correspond to up/down flows. The large value $+24 \text{ km s}^{-1}$ corresponds to the speed of a rising bubble from the limb or the flow speed of its bright edge. Fine threads close to the limb are spicules. Wave pattern corresponds to oscillations with 15 to 20 min of period. Adjacent pixels in a slice have coherent velocities.

der of a few km s^{-1} to 6 km s^{-1} reaching 11 km s^{-1} for individual fine threads. The pattern of the Dopplershift map show elongated cells nearly perpendicular to the limb. They are **wider than the MSDP spatial resolution**. The time slice maps exhibit several pixels close to each other along the slice having a similar velocity trend. This means that fine threads close to each other have a coherent displacement. According to the observations of the prominence three days before when it is still on the disk as a filament, it appears that only the feet or barbs are enough dense to be observed. The prominence would represent the barb threads integrated along the line-of-sight as the filament is crossing the limb. The structures are not vertical in the sky plane (x,z) as suggested by the movie. Dopplershifts and transverse velocities are of same order of magnitude (less than 6 km s^{-1}). In Table 1 we

have selected individual threads with the largest transverse velocities in region with higher Dopplershifts. The other parts of the prominence exhibit coherent velocity much smaller (1 to 2 km s^{-1}) difficult to measure. The narrow profiles of $H\alpha$ lines of the prominence indicate that the different threads integrated along the line of sight have similar velocities. The dispersion of the velocities along the line-of-sight is small.

The longitudinal magnetic field observed (by the SOHO/MDI instrument) in the filament channel on the disk and on both edges of the inversion line is weak. The strength of the small polarities are less than 10 Gauss. The prominence lies in a quiet region and corresponds to a quiescent filament. The small polarities can change rapidly and this would explain the fast dynamics of the structures.

In a flux tube model (Aulanier & Démoulin, 1998; Dudík et al., 2008) the $H\alpha$ filament is considered as cool material trapped in shallow dips along long magnetic field lines. The feet are extension of the flux tube disturbed laterally by parasitic polarities. The barbs are piled up dips touching the photosphere. When a parasitic polarity cancels or moves, the feet move and can even disappear (Aulanier et al., 1998; Schmieder et al., 2006; Gosain et al., 2009). **In this 3D perspective the prominence material would be trapped in inclined field lines and the downflow motion would occur along the shallow dips. The brightness would result of the integration of the threads along the line-of-sight (see Fig. 3e in Dudík et al., 2008).** Aulanier et al. (1998) explain very well through their magnetic extrapolation the relationship between parasitic polarities and the flux tube itself and their evolution. The flux of parasitic polarity overcomes that of the twisted flux tube and destroys the twisted configuration. The bubbles would be structures more magnetized than the surrounding and represented by the separatrices. A small increase of magnetic pressure in the bubble would lead to the rise of it in the atmosphere. Strong currents can be created in the quasi separatrix layers (QSL) around the separatrices by photospheric displacements of the parasitic polarities (Démoulin et al., 1996). Energy release is expected. This could correspond to the brightening **ribs** associated with filaments (Heinzel et al., 1995). They are not systematically visible due to the dense plasma of filaments. In SOT observations it could correspond to the bright top edge of the cavities where reconnection could occur and expel plasma. This would explain the fast velocity material in brighter threads surrounding the dark cavities. On the next days, such bubbles are not observed in the prominence because the feet and parasitic polarities related to it would be on the back side of the disk. **In the arcade model with dips proposed by Heinzel & Anzer (2001) the prominence observed on April 25 may would consist of vertical threads trapped in dips and piled up giving the impression of vertical continuous threads. The downflows of 1 to 5 km s^{-1} would be due to shrinkage or successive reconnections of field lines.**

Another explanation for the buoyancy of the dark cavities or bubbles could be adiabatic expansion of a heated volume of plasma (Berger et al., 2008). This is not exclusive of the magnetic pressure increase scenario and both magnetic and thermal buoyancy may play a role in the formation of these structures. We would like to measure the magnetic field in the bubbles and in the prominence. An interesting aspect would be also to analyse the EIS and SUMER data to see if the dark bubbles are filled with hot material. Such measurements are needed to know which mechanism is valid for the formation of these dark low cavities.

Acknowledgements. We thank Nicolas Labrosse the chief planner of JOP 178 during the Hinode-SUMER campaign at MEDOC, operating center in Orsay

who forecasted the correct pointing of this prominence three days in advance. We thank T. E. Berger of the Lockheed Martin Solar and Astrophysics Laboratory for processing the *Hinode*/SOT data and for correcting the English language of the manuscript. R.C. thanks the CEFIPRA for his post-doctoral grant. This work is done in the frame of the European network SOLAIRE. We would like to thank the *Hinode* science team for the observations of SOT, the Meudon solar tower team for the MSDP observations particularly G. Molodij. We thank Guo Yang for his help in developing the time-slice procedure. The work of A.B. was supported by the Polish Ministry of Science and Higher Education (grant N203 016 32/2287), by the Academy of Sciences of the Czech Republic (grant M100030942) and the Observatoire de Paris. *Hinode* is a Japanese mission developed and launched by ISAS/JAXA, collaborating with NAOJ as a domestic partner, NASA and STFC (UK) as international partners.

References

- Aulanier, G. & Démoulin, P. 1998, *A&A*, 329, 1125
- Aulanier, G., Démoulin, P., van Driel-Gesztelyi, L., Mein, P., & Deforest, C. 1998, *A&A*, 335, 309
- Berger, T. E., Shine, R. A., Slater, G. L., et al. 2008, *ApJ*, 676, L89
- Chae, J., Ahn, K., Lim, E.-K., Choe, G. S., & Sakurai, T. 2008, *ApJ*, 689, L73
- David, K.-H. 1961, *Zeitschrift für Astrophysik*, 53, 37
- d’Azambuja, L. & d’Azambuja, M. 1948, *Ann. Obs. Paris-Meudon*, 6, 7
- Démoulin, P., Hénoux, J. C., Priest, E. R., & Mandrini, C. H. 1996, *A&A*, 308, 643
- Démoulin, P., Malherbe, J. M., & Priest, E. R. 1989, *A&A*, 211, 428
- Dudík, J., Aulanier, G., Schmieder, B., Bommier, V., & Roudier, T. 2008, *Sol. Phys.*, 248, 29
- Gosain, S., Schmieder, B., Venkatakrishnan, P., Chandra, R., & Artzner, G. 2009, *Sol. Phys.*, 259, 13
- Gouttebroze, P., Heinzel, P., & Vial, J. C. 1993, *A&AS*, 99, 513
- Gunár, S., Heinzel, P., Schmieder, B., Schwartz, P., & Anzer, U. 2007, *A&A*, 472, 929
- Heinzel, P. & Anzer, U. 2001, *A&A*, 375, 1082
- Heinzel, P., Anzer, U., & Gunár, S. 2005, *A&A*, 442, 331
- Heinzel, P., Kotrč, P., Mouradian, Z., & Buyukliev, G. T. 1995, *Sol. Phys.*, 160, 19
- Heinzel, P., Schmieder, B., Fárnik, F., et al. 2008, *ApJ*, 686, 1383
- Karpen, J. T., Antiochos, S. K., Klimchuk, J. A., & MacNeice, P. J. 2003, *ApJ*, 593, 1187
- Karpen, J. T., Tanner, S. E. M., Antiochos, S. K., & DeVore, C. R. 2005, *ApJ*, 635, 1319
- Kippenhahn, R. & Schlüter, A. 1957, *Zeitschrift für Astrophysik*, 43, 36
- Kosugi, T., Matsuzaki, K., Sakao, T., et al. 2007, *Sol. Phys.*, 243, 3
- Kuperus, M. & Raadu, M. A. 1974, *A&A*, 31, 189
- Labrosse, N., Heinzel, P., Vial, J. C., et al. 2009, *Space Science Reviews* (in press)
- Lin, Y., Engvold, O., Rouppe van der Voort, L., Wiik, J. E., & Berger, T. E. 2005, *Sol. Phys.*, 226, 239
- Lin, Y., Engvold, O. R., & Wiik, J. E. 2003, *Sol. Phys.*, 216, 109
- Mackay, D. H., Karpen, J. T., Ballester, J. C., Schmieder, B., & Aulanier. 2009, *Space Science Reviews* (in press)
- Malherbe, J. M. 1989, in *Dynamics and Structure of Quiescent Solar Prominences*, ed. E. R. Priest (Kluwer Academic Press.), 115
- Mariska, J. T. & Poland, A. I. 1985, in *Bulletin of the American Astronomical Society*, Vol. 17, 842
- Mein, P. 1977, *Sol. Phys.*, 54, 45
- Mein, P. 1991, *A&A*, 248, 669
- Mein, P. & Mein, N. 1991, *Sol. Phys.*, 136, 317
- Okamoto, T. J., Tsuneta, S., Berger, T. E., et al. 2007, *Science*, 318, 1577
- Saito, K. & Tandberg-Hanssen, E. 1973, *Sol. Phys.*, 31, 105
- Schmieder, B. 1989, in *Dynamics and Structure of Quiescent Solar Prominences*, ed. E. R. Priest (Kluwer Academic Press.), 15
- Schmieder, B., Aulanier, G., Mein, P., & López Ariste, A. 2006, *Sol. Phys.*, 238, 245
- Schmieder, B., Bommier, V., Kitai, R., et al. 2008, *Sol. Phys.*, 247, 321
- Schmieder, B., Raadu, M. A., & Wiik, J. E. 1991, *A&A*, 252, 353
- Tandberg-Hanssen, E. 1994, in *The nature of solar prominences* (Kluwer Academic Press.), 113–165
- Török, T., Aulanier, G., Schmieder, B., Reeves, K. K., & Golub, L. 2009, *ApJ*, 704, 485
- van Ballegooijen, A. A. & Martens, P. C. H. 1989, *ApJ*, 343, 971
- Zirker, J. B., Engvold, O., & Martin, S. F. 1998, *Nature*, 396, 440